

Journal of Alloys and Compounds, 536S1 (2012) 550-553

<http://dx.doi.org/10.1016/j.jallcom.2011.11.109>

Analysis of nanocrystallization kinetics and crystal size distribution under limited growth approach

J.S. Blázquez*, C.F. Conde, A. Conde

Dpto. Física de la Materia Condensada. ICMSE-CSIC. Universidad de Sevilla. P.O. Box 1065. 41080-Sevilla (Spain)

Abstract

Two different simulation approaches have been used to describe nanocrystallization processes: a limited growth approach, which is an extension from instantaneous growth approximation, and an average soft impingement simulation where spherical crystallites grow to a size for which the corresponding region depleted in Fe (or the element enriched in crystalline phase) is comparable to the average distance between them. Both simulations agree describing a local Avrami exponent which decreases down to ~ 1 as crystallization fraction increases. Experimental data for evolution of crystal size and crystal size distribution are reproduced.

Keywords: Nanocrystallization kinetics; cellular automata; Avrami exponent.

Departamento de Física de la Materia Condensada. Universidad de Sevilla.

Apartado 1065, 41080 Sevilla (Spain).

Phone: (34) 95 455 60 29/ Fax: (34) 95 461 20 97

E-mail: jsebas@us.es

1. Introduction

In nanocrystalline microstructures, the fact that structural length becomes at the scale of the characteristic lengths of several physical properties leads to new phenomenologies in these systems, different to that exhibited by bulk samples with micrometric crystals. Nanocrystalline microstructures can be obtained directly from the melt, e.g. by rapid quenching, or by ball milling. However, crystallization of a precursor amorphous alloy allows for a finer control of the final microstructure. Therefore, the strong interplay between microstructure and properties makes very interesting the study of the crystallization kinetic processes involved.

Nanocrystallization kinetics exhibits several characteristics which make difficult its interpretation in the frame of the classical theory of crystallization of Johnson, Mehl, Avrami and Kolmogorov (JMAK) [1]. Different approximations have been developed to solve this problem: soft impingement [2], modification of JMAK theory including an impingement factor [3] or instantaneous growth approach [4]. The latter, developed by the authors, has been extended to a limited growth approach [5] considering a transient time after nucleation of interface controlled growth followed by growth blocking. The resulting Avrami exponents for limited growth indicate that, although some crystals grow at any time, the global kinetics can be interpreted only due to nucleation even for polymorphic transformations.

In this work, limited growth approach is analyzed using two different simulation models: crystallization of a space divided in cubic cells (Cell-Sim) [5,6] and crystallization of a continuous space (Cont-Sim) where an average soft impingement is considered. Both assume the formation of a Fe rich crystalline phase. However, generalization to other compositions is straightforward.

2. Simulation programs

2.1 Simulation of a 3D space divided on cubic cells

This simulation program (Cell-Sim) is detailed elsewhere [5] and, therefore, a simple description is given here. The cellular automata created considers a three dimensional space divided in cubic cells and the time is discretized in iteration steps. Every time unit a cell is randomly chosen to crystallize if several deterministic (the cell must be amorphous and have enough Fe in its neighbourhood) and stochastic (a probability for nucleation is assigned related to the composition) are fulfilled. During the time unit, all the crystallites below certain size are allowed to grow to those neighbour cells which are not already crystallized and could be enriched in the needed element from their surroundings.

2.2 Simulation of a continuous space

In this new simulation (Cont-Sim) the explored volume is equal to a sphere of radius L . The time is discretized as in the previous simulation in iteration steps. Fe crystals are assumed to be spherical and for each crystal there are two radii to take into account: radius R , which corresponds to that of the crystal, and radius $R_2 > R$, which corresponds to a larger sphere surrounding the crystal which is depleted in Fe.

The R_2 radius is calculated using a Zener compositional profile [7] being equal to $R_2 = R \left(\frac{2c_x - c_i - c_e}{c_i - c_e} \right)^{1/3}$, where c_x is the Fe composition of the crystalline phase, c_i is

the Fe composition of the initial amorphous phase and c_e is the equilibrium Fe

composition at the crystal/amorphous interface. Besides the crystalline fraction,

$X_C = \frac{\sum_i R(i)^3}{L^3}$, a fraction of volume excluded from crystallization is defined as

$X_{Exc} = \frac{\sum_i R_2(i)^3}{L^3}$. This fraction determines the region where new nuclei cannot be

formed and nucleation probability is thus proportional to $1-X_{Exc}$. In the previous simulation, once a new cell is chosen for nucleation and after checking if it is amorphous (with a probability $1-X_C$) a probability ascribed to the Fe enrichment needed must be also overcome to allow the new nucleus for developing a new crystal. In the present simulation, this probability is related to $(c_x-c_i)/c_x$ and it remains constant during the process as the composition of the whole region allowed to crystallize is homogenous and equal to c_i .

During each iteration step (time unit), every crystal will increase its radius R to $R+dR$ except for those crystallites with a radius of the corresponding affected region,

R_2 , larger than half the average distance between crystallites, $d = L\left(\frac{4\pi}{3N}\right)^{1/3}$, where N is

the number of crystals formed. Those crystals will remain blocked in a similar way as the limited growth mechanism described by the previous simulation does, although, unlike for Cell-Sim, the growth stop is a consequence of soft impingement.

In this new continuous space simulation, information of crystal localization is lost and both geometrical and soft impingements are considered on average. However, the effects of cubic shape of cells are overcome (anisotropic growth, deviation from expected linear growth). In the previous work this was afforded by analyzing the evolution of the volume of the crystal [5].

For both simulations, linear growth is proportional to iteration steps, describing an interface controlled process meanwhile the crystal is allowed to grow. The step function of such growth rate can be considered as an approximation to the actual growth rate described by an initial interface controlled growth followed by diffusion controlled growth for a primary phase growing in a supersaturated matrix (see Fig. 3 in ref. [2]).

A comparison between the relevant parameters of both simulation programs describing limited growth is shown in table 1.

3. Results and discussion

As a starting point it is important to establish the differences between the growth of a single grain in Cell-Sim and Cont-Sim. As it was shown earlier [5], a crystal growing in Cell-Sim will reduce the exponent of growth from 3 to 0 as the initial Fe content of the system is decreased due to the limited region from which the crystallizing cells are allowed to get Fe, indirectly considering diffusion processes. However, in Cont-Sim, a single crystal will grow freely with a growth exponent equal 3 till its affected sphere equals $\sim 1/2$ of the explored volume and suddenly it stops growing. Thus purely interface controlled growth is considered meanwhile growth is allowed.

Figure 1 shows the evolution of the crystalline fraction, X_C , average radius of crystals, $\langle R \rangle$, number of crystals, N , and average distance between crystals, $\langle d \rangle$, for different simulated binary compositions $\text{Fe}_x\text{A}_{100-x}$, where A is assumed to be an element insoluble in the bcc Fe crystals in Cont-Sim frame ($L=1000$, $dR=1$). In all the simulations shown $c_e=0$. As the Fe content increases in the composition, the crystalline fraction at saturation increases (smaller values could be obtained tailoring c_e). It can be

observed that crystal size saturation is achieved much earlier than saturation in crystalline fraction and that nucleation occurs till the final stages of the process. These characteristics are typical for nanocrystallization processes and yield the instantaneous growth approximation [6].

The analysis of crystalline fraction evolution in the frame of JMAK theory yields the local Avrami shown in figure 2. These values were calculated as:

$$n(X) = \frac{d \ln[-\ln(1-X)]}{d \ln(t-t_0)},$$
 where t is the time (iteration step), t_0 is the incubation time

(zero in our case) and X is the transformed fraction. If X is not properly normalized but X_C is used instead, some apparent differences appear between the different compositions. However, if X is normalized to 1 at the end of the transformation (as shown in figure 2 above) the curves almost collapse in a single behaviour independent of composition and nucleation rate chosen (assuming the explored space is not so small that artefacts appear). This is an intrinsic behaviour of a system crystallizing under the average impingement described and results indicate that it cannot be properly described by JMAK theory. Geometrical impingement considered in JMAK theory allows anisotropic growth, as well as Cell-Sim, but the average soft impingement used in Cont-Sim simulation blocks the volume growth of spherical crystals (not only a linear growth). This fact is consistent with the regular shaped crystals found in some nanocrystalline samples. The general behaviour of the local Avrami exponent obtained in Cont-Sim can be described as following. Initially, when there is no impingement in growth and nucleation is not seriously affected $n(X)$ slightly increases above 4, which should correspond to a constant nucleation and three dimensional interface controlled growth. These abnormally high values deserve some explanation. Geometrical impingement in JMAK theory affects growth since the very beginning of the process.

However, average soft impingement is statistically relevant only for a significant number of crystallites. Therefore, the results for X below ~ 0.2 should be neglected. For larger values of X , n decreases down to ~ 1 , as it occurs for nanocrystallization processes. Similar results could be obtained in the frame of Cell-Sim [5]. An example is shown in figure 3 for the local Avrami exponent obtained for the crystallization of $\text{Fe}_{75}\text{A}_{25}$ alloy in a $50 \times 50 \times 50$ cells space using different limits for growth. The advantage of Cont-Sim is that growth limitation is a consequence of the evolution of the system, unlike for Cell-Sim, where it is an initial parameter of the simulation.

The Cont-Sim simulation can supply information of the evolution of crystal size distribution during crystallization. Figure 4 shows histograms obtained at different crystalline fractions for $\text{Fe}_{75}\text{A}_{25}$ alloy in the same conditions of figures 1 and 2.

Finally, experimental data have been reproduced for $\text{Fe}_{60-x}\text{Co}_x\text{Nb}_6\text{B}_{16}$ alloy series ($x=18, 39$ and 60). In the case of $x=18$ alloy, nanocrystallization stops due to Fe exhaustion of the matrix, thus $c_e=0$ has been used. As far as the excluded fraction is not exhausted in Fe at the end of the simulation, the crystalline fraction has been rescaled. On the other hand, radii obtained in the simulations are in arbitrary units, thus they have been also rescaled. Table 2 summarizes the main results. In order to reproduce the relative variation of the data between the three compositions, c_e has been tuned. The estimated values are ~ 15 and ~ 35 for $x=39$ and 60 , respectively. This implies that the concentration of Fe+Co at the interface is similar for the three samples ($60, 54$ and 53 for $x=18, 39$ and 60 , respectively).

4. Conclusions

Soft impingement has been simulated in a continuous space where the spherical crystals grow till the size of the sphere depleted in Fe surrounding a crystal is comparable to the average distance between crystallites. With this simple premise, qualitative behavior of crystallite size evolution and local Avrami exponent of nanocrystallization processes is reproduced. Moreover, in this frame, a limited growth can be predicted which is complementary to previous simulations under limited growth approach.

Acknowledgements

This work was supported by the Spanish Ministry of Science and Innovation (MICINN) and EU FEDER (project MAT2010-20537) and the PAI of the Regional Government of Andalucía (project FQM-6462).

Table 1. Relevant parameters for the two simulations used describing limited growth.

	Cubic cells	Continuous space
Volume explored	Parallelepiped: L_x, L_y, L_z	Volume of a sphere of radius L
Interface controlled growth	Crystal grows to neighbor cells each iteration step	Crystal grows dR each iteration step
Nucleation rate, I	Proportional to $(1-X_C):f_{nuc}$, being f_{nuc} dependent of cell composition	Proportional to $(1-X_{Exc})$ Composition of nucleation regions is homogeneous and equal to c_i .
In both cases reducing explored volume enhances I		
Region affected by crystals	The cubic cell acquires Fe from the amorphous cells of its six neighbor cells as $6fV_{cell}$, being $f < 1$ user defined.	Defined by Zener diffusional profile: $R_2 = R \left(\frac{2c_x - c_i - c_e}{c_i - c_e} \right)^{1/3}$ User controlled through c_e
Growth limit defined by:	User and geometrical impingement	Soft impingement: $R_2 < \frac{L}{2} \left(\frac{4\pi}{3N} \right)^{1/3}$

Table 2. Crystalline fraction, X_C , and average crystal radii, $\langle R \rangle$ from experiment (exp) and simulation (sim) along with the equilibrium concentration of Fe at the interface, c_e , used in the experiments.

X (%)	$X_C(\text{exp})$ [8]	$\langle R \rangle(\text{exp})$ [9] (nm)	$X_C(\text{sim})$	$X_C(\text{exp})/X_C(\text{sim})$	$\langle R \rangle(\text{sim})$	$\langle R \rangle(\text{exp})/\langle R \rangle(\text{sim})$	c_e
18	0.43	4.5	0.29	1.5	88	0.051	0
39	0.53	4.5	0.35	1.5	107	0.042	15
60	0.54	5.0	0.36	1.5	100	0.050	35

Figure captions

Figure 1. Crystalline fraction, X_C , average radius of crystals, $\langle R \rangle$, number of crystals, N , and average distance between crystals, $\langle d \rangle$, for different simulated binary compositions $\text{Fe}_x\text{A}_{100-x}$ as a function of the iteration step (time).

Figure 2. Local Avrami exponent from Cont-Sim using X_C and normalizing the transformed fraction.

Figure 3. Local Avrami exponent from Cell-Sim normalizing the transformed fraction for different binary compositions.

Figure 4. Histograms for the crystal size distributions obtained from Cont-Sim at different iteration steps.

Figure 1

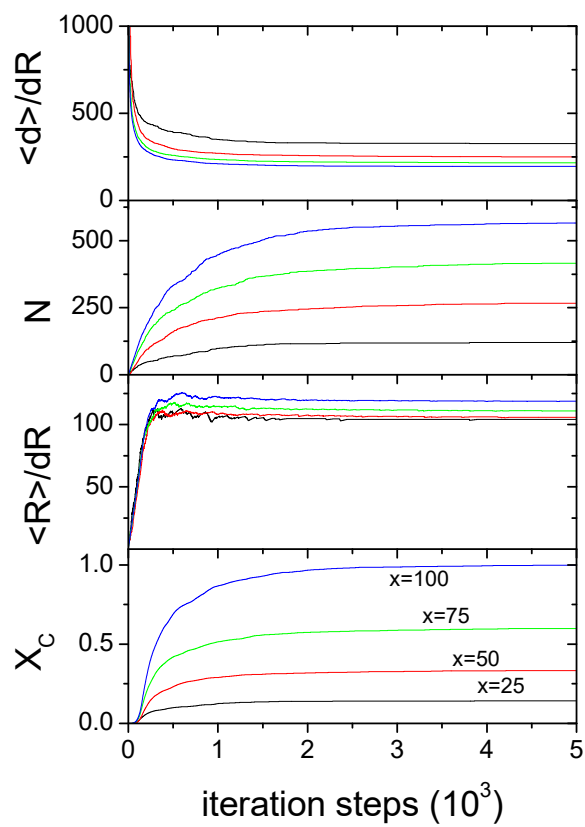


Figure 2

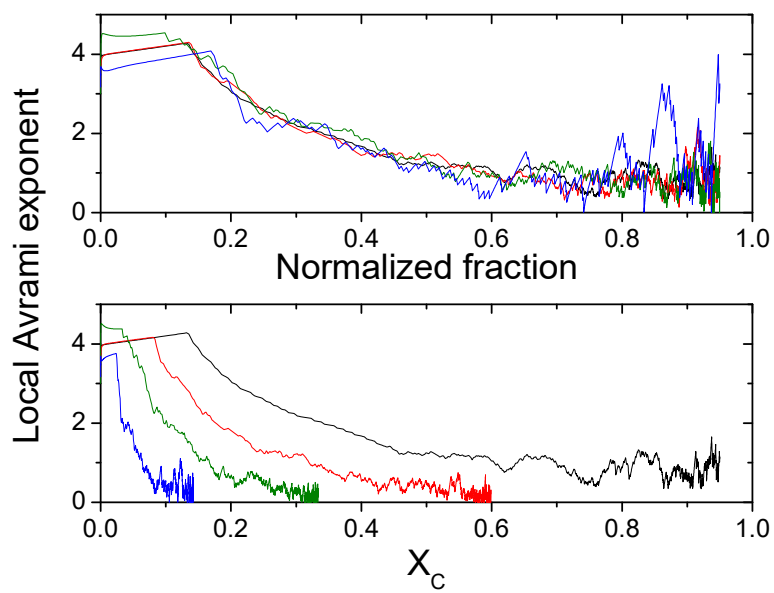


Figure 3

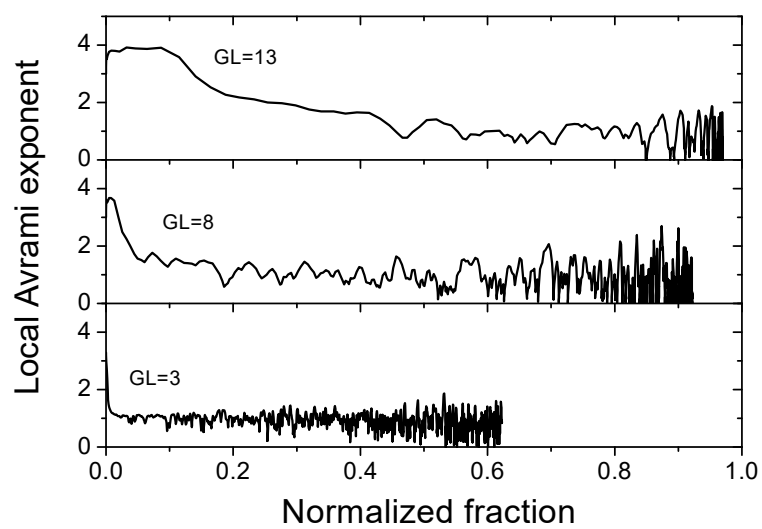
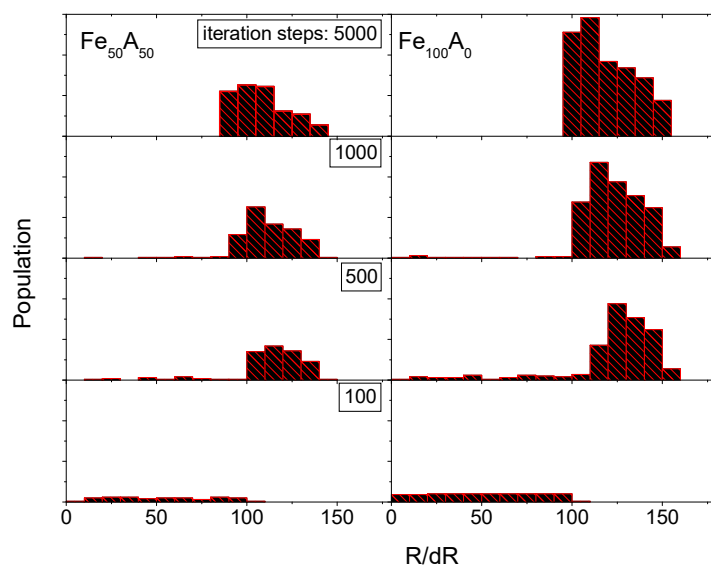


Figure 4



References

-
- [1] K. Barmak, *Metal. Mater. Trans. B* (DOI: 10.1007/s11663-010-9421-1)
- [2] M. T. Clavaguera-Mora, N. Clavaguera, D. Crespo, T. Pradell, *Prog. Mater. Sci.* 47 (2002) 559.
- [3] M. J. Starink, *J. Mater. Sci.* 36 (2001) 4433.
- [4] J.S. Blázquez, M. Millán, C.F. Conde, A. Conde, *Phil. Mag.* **87** (2007) 4151.
- [5] J.S. Blázquez, C.F. Conde, A. Conde, *J. Non-Cryst. Solids* 357 (2011) 2833.
- [6] J.S. Blázquez, C.F. Conde, A. Conde, *J. Non-Cryst. Solids* 354 (2008) 3597.
- [7] J. Burke, *The kinetics of phase transformations in metals*, Pergamon Press, 1965, Oxford, p. 166.
- [8] J. S. Blázquez, V. Franco, C. F. Conde, A. Conde, *J. Mag. Mag. Mat.* 254-255 (2003) 460.
- [9] J. S. Blázquez, V. Franco, A. Conde, *J. Phys.: Cond. Matter* 14 (2002) 11717.